

High-Resolution Modeling of Summertime Biogenic Isoprene Emissions in New York City

Dandan Wei,* Cong Cao, Alexandra Karambelas, John Mak, Andrew Reinmann, and Róisín Commane

Cite This: <https://doi.org/10.1021/acs.est.4c00495>

Read Online

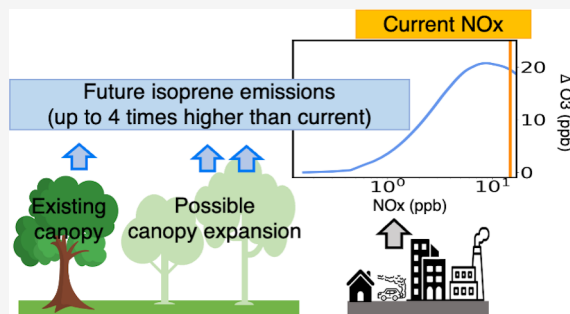
ACCESS |

Metrics & More

Article Recommendations

ABSTRACT: As cities strive for ambitious increases in tree canopy cover and reductions in anthropogenic volatile organic compound (AVOC) emissions, accurate assessments of the impacts of biogenic VOCs (BVOCs) on air quality become more important. In this study, we aim to quantify the impact of future urban greening on ozone production. BVOC emissions in dense urban areas are often coarsely represented in regional models. We set up a high-resolution (30 m) MEGAN (The Model of Emissions of Gases and Aerosols from Nature version 3.2) to estimate summertime biogenic isoprene emissions in the New York City metro area (NYC-MEGAN). Coupling an observation-constrained box model with NYC-MEGAN isoprene emissions successfully reproduced the observed isoprene concentrations in the city core. We then estimated future isoprene emissions from likely urban greening scenarios and evaluated the potential impact on future ozone production. NYC-MEGAN predicts up to twice as much isoprene emissions in NYC as the coarse-resolution (1.33 km) Biogenic Emission Inventory System version 3.61 (BEIS) on hot summer days. We find that BVOCs drive ozone production on hot summer days, even in the city core, despite large AVOC emissions. If high isoprene emitting species (e.g., oak trees) are planted, future isoprene emissions could increase by 1.4–2.2 times in the city core, which would result in 8–19 ppbv increases in peak ozone on ozone exceedance days with current NO_x concentrations. We recommend planting non- or low-isoprene emitting trees in cities with high NO_x concentrations to avoid an increase in the frequency and severity of future ozone exceedance events.

KEYWORDS: isoprene, ozone, air quality, urban greening, high-resolution, MEGAN, NYC



INTRODUCTION

Volatile organic compounds (VOCs) are reactive chemicals emitted into the atmosphere from anthropogenic and biogenic sources. In urban regions with elevated concentrations of nitrogen oxides (NO_x), VOCs can undergo photochemical reactions leading to the formation of ground-level ozone, which has adverse effects on human health and ecosystems.^{1,2} The sensitivity of ozone formation to precursor emissions is typically classified as NO_x- or VOC-limited. Ozone chemistry still remains VOC-limited in all seasons in urban cores of major US cities (such as New York City, Los Angeles, and Chicago)^{3–6} even as NO_x reduction policies have turned the surrounding areas NO_x-limited in summer over the past decades.⁷ Quantitative attribution of ozone formation to VOCs from various emission sources is needed to design effective control measures.

VOCs come from two major sources, anthropogenic volatile organic compounds (AVOCs) emitted from human activity and biogenic volatile organic compounds (BVOCs) emitted from terrestrial ecosystems with isoprene accounting for almost half of all BVOC fluxes globally.⁸ The influences of AVOCs on urban atmospheric chemistry have been extensively studied

through source apportionment.^{9–13} BVOCs, which have received less attention, play an important role in urban atmospheric chemistry due to their higher chemical reactivity compared to many AVOCs. Churkina et al.¹⁴ found that BVOCs contribute to 40–60% of ground-level ozone formation on hot summer days in Berlin, Germany. Coggon et al.¹⁵ suggested that BVOCs were a major contributor to ozone in the New York City metropolitan area during a pollution episode in 2018. Ma et al.¹⁶ illustrated that increases in BVOC emissions due to urban greening between 2003 and 2016 increased maximum daily 8 h ozone concentration by 9% during a heatwave event in Beijing, China. Gu et al.¹⁷ predicted that doubling urban green space with high-isoprene emitting species can lead to a relative change in ozone formation potential of 185.4% in Los Angeles, US. Schlaerth et al.¹⁸

Received: January 15, 2024

Revised: June 17, 2024

Accepted: June 20, 2024

showed that a 50% increase in vegetation cover of high isoprene emissions leads to 1.25 ± 1.11 ppbv increases in daily maximum 8 h ozone concentrations in urban areas in Southern California. As cities strive for both ambitious reductions in AVOC emissions and increases in tree canopy cover, accurate assessments of the impacts of BVOCs on air quality become more important.

The Model of Emissions of Gases and Aerosols from Nature (MEGAN) is the most frequently used empirical model for BVOC emission estimation.¹⁹ MEGAN is driven by land cover, tree species composition, plant leaf phenology, and meteorological data and can be run at user defined spatial resolutions.²⁰ High uncertainties in the calculation of BVOC emissions are associated with the representation of land covers by satellite-based products on global and regional scales.²¹ Due to heterogeneity in land cover, high spatial resolution biosphere models (2 m to 500 m) are required to adequately simulate urban ecosystem fluxes for street trees and fragmented urban forests.^{22–24} Thereby, accurate estimation of BVOC emissions within urban areas needs higher resolution data.

The New York City (NYC) metropolitan area continues to persistently violate the federal health-based air quality standards for ground-level ozone during hot summer days.^{25,26} Ozone concentrations exhibit significant variations both vertically (>40 ppbv over short distance²⁷) and horizontally (>15 ppbv per km²⁶) around NYC. Studies using Chemical Transport Models (CTMs), providing spatial and temporal representations of atmospheric conditions, have been focused on the impacts of meteorology and local AVOC emissions on ozone production in the NYC metropolitan area.^{15,26,27} However, the local BVOC fluxes in NYC are coarsely represented in CTMs (>1 km) and are likely underestimated.²⁵ A recently released high-resolution (15 cm) land cover map,²⁸ tree survey data,²⁹ and 30 m Landsat phenology data³⁰ make high-resolution modeling of BVOCs for NYC possible, which will contribute to better spatial and temporal representation of urban biosphere in CTMs.

NYC established a citywide goal of equitably reaching at least 30% tree canopy cover by 2035 (The New York City Council, Int 1066–2023) motivated by the ecosystem services provided by trees (e.g., CO₂ mitigation,³¹ water interception,³² and heat mitigation³³) as well as by city beautification and increased property values. Treglia et al.³⁴ suggest the existing NYC landscape could support 159 km² of additional tree canopy, doubling the current canopy cover of 22% (as of 2017) to 42% of the land area. There is rapidly growing interest among urban planners to favor planting native species because they support native biodiversity. In New York City, oak (*Quercus* spp.) and sweetgum (*Liquidambar styraciflua*) trees, in particular, are native genera often favored because they are also considered to be climate resilient trees that are more likely to survive under changing climate conditions such as hotter drier summers and wetter warmer winters. However, oaks and sweetgum are major isoprene-emitting genera, and it is critically important to assess how the tree species used for increasing canopy cover might influence urban atmospheric chemistry.

The research question of this study is “Will urban greening impact air quality in NYC?” To answer the question, we set three objectives: (i) provide a modeling framework informed by high-resolution land cover maps to estimate BVOC emissions in urban areas; (ii) determine the contribution of BVOCs to ozone formation using an observation-constrained

box model; (iii) evaluate the potential impacts of future urban greening strategies on ozone production. Monoterpenes are primarily from fragranced volatile chemical products and other anthropogenic sources in the NYC metropolitan area.¹⁵ We focus on isoprene in this study because of its potential predominance among BVOCs in NYC and high reactivity toward ozone, although the modeling framework is capable of simulating other BVOC species.

METHODOLOGY

NYC-MEGAN. Study Site. The study domain covers a rectangular geographic area of 2171 km² centered on NYC. The domain includes the five boroughs of NYC (Manhattan, Bronx, Queens, Brooklyn, and Staten Island) and part of the surrounding suburbs. The suburbs include part of New Jersey to the west of the domain, part of Westchester County, NY to the north, and part of Nassau County, NY to the east (Figure 4a). Roughly 30% of the domain area is water. We set up a 30 m MEGAN for the study domain. Hereafter, we refer to the model as NYC-MEGAN. Because the 15 cm land cover map and tree species composition data are only available for the five boroughs of NYC (see details in Input Data), we base our results and discussion on the five boroughs of NYC for accuracy, although we show the results for the rest of the domain in the figures. We refer to the five boroughs of NYC as NYC. The total land area of NYC is 778.18 km².

Input Data. The equations used in the NYC-MEGAN can be found in eqs 1–19 in Guenther et al.⁸ We used the species-specific emission factors (i.e., the emission flux from a particular vegetation type per unit area under standard conditions) compiled for the original MEGAN (<https://ba.ess.uci.edu/megan/data-and-code/megan32>). Other input data came from publicly available data sets including the 15 cm land cover map, tree survey data, 30 m leaf area index (LAI), photosynthetically active radiation (PAR), and air temperature (T_a).

The 15 cm spatial resolution land cover map for NYC (<https://data.cityofnewyork.us/Environment/Land-Cover-Raster-Data-2017-6in-Resolution/he6d-2qns>) was used to derive the 30 m spatial resolution vegetation covers (i.e., tree, herb, shrub, and crop covers). Note that the 15 cm land cover map is only available for NYC. We used the 30 m national Land cover database (NLCD) 2021 tree cover (<https://www.mrlc.gov/data/nlcd-2021-usfs-tree-canopy-cover-conus>) for areas outside NYC. The urban forest survey²⁹ found little shrub area in NYC. We assumed zero shrub and crop cover for the rest of the study domain outside NYC. We derived herb cover for areas outside NYC via deducting the combined NLCD tree cover and impervious cover³⁵ from each pixel. We considered two types of urban ecosystems in the model, namely, street trees and park trees (see details in Tree Species Composition). Tree species composition for street trees was based on the 2015–2016 street tree census (<https://www.nycgovparks.org/trees/treescount>) that located and counted every street tree in NYC (666,134 in total) and recorded their attributes (e.g., species and diameters). The urban forest survey²⁹ that covered the public parks and urban forests was used to obtain the tree species composition for park trees and trees in urban forests. Note that private gardens are not included in the tree species composition due to lack of data. The street tree census and urban forest survey are only available for NYC. We assumed the tree composition is the same for the rest of the study domain outside NYC. The 30 m

resolution LAI data were derived using a data-driven method³⁰ on Google Earth Engine. Both the 16-day Landsat 7 and 8 retrievals were used to create an 8-day data set of LAIs. The 8-day LAIs were then interpolated into daily values using a cubic spline function. The PAR and Ta were extracted from the High-Resolution Rapid Refresh HRRR,³⁶ a NOAA real-time 3 km resolution, hourly updated atmospheric model. The HRRR 2D Surface Levels analysis product was used. The 3 km PAR and Ta were linearly resampled into 30 m spatial resolution to match the other input data.

NYC-MEGAN produces BVOC emissions at a spatial resolution of 30 m and a temporal resolution of 1 h. We ran NYC-MEGAN for July 2018. We selected an ozone exceedance day (July 2, 2018, high was 35 °C) to show the 30 m modeled isoprene emissions across NYC. We also show the monthly total isoprene emissions for each borough. We also ran NYC-MEGAN for ozone exceedance days in July 2020 for the evaluation against trace gas observations in Manhattan in 2020.

We compared the 30 m spatial resolution isoprene emissions from NYC-MEGAN with the 1.33 km Biogenic Emission Inventory System version 3.61 (BEIS) to assess how higher spatial resolution land cover impacts estimation of isoprene emissions (Figure 4b,d). BEIS is another global biogenic inventory widely used for scientific and regulatory purposes. BEIS relies on the Biogenic Emission Land use Database version 4 (BELD), which includes Moderate Resolution Imaging Spectroradiometer (MODIS) land use data, 2006 NLCD land cover, US Forest Service Forest Inventory and Analysis vegetation data, and the 2007 US Department of Agriculture agriculture data census.³⁷ BEIS was run in-line with the coupled Weather Research and Forecasting (version 4.1.1)–Community Multiscale Air Quality Modeling System (version 5.3.1) model,³⁸ and hourly output was saved. The physical schemes used in the WRF–CMAQ runs are described in detail in Torres-Vazquez et al.³⁸

Limitation and Uncertainties of the NYC-MEGAN. NYC-MEGAN provides a modeling framework informed by high-resolution land cover maps to estimate BVOC emissions in urban areas. However, there are a number of limitations that will contribute to the total uncertainty due to lack of information: (i) we only consider trees in public areas such as streets and parks. The private space such as backyards are missing, potentially leading to underestimation of isoprene emissions; (ii) tree species composition is not spatially resolved, so NYC-MEGAN might not capture full spatial distribution of street- or park-level isoprene emissions; (iii) urban trees undergo different levels of stress depending on their location and ecosystems. We may be under- or overestimating isoprene fluxes. Future studies should investigate BVOC emissions from stressed urban trees; (iv) urban canopy environments (e.g., shading, fragmented, etc.) are not considered in NYC-MEGAN, due to lack of information; (v) the linear resampling of the 3 km PAR and Ta to 30 m does not incorporate surface influences at fine spatial resolutions that may change the temperature and PAR, such as building materials and heights, street canyon depths, surface impermeousness, vegetation cover, and proximity to water bodies. Not incorporating these fine spatial resolution effects may lead to an underestimate in the spatial variability of the simulated BVOC emissions.

Box Modeling. To calculate the isoprene concentrations and compare them with the measurements, we set up a box

model incorporating the isoprene emissions from NYC-MEGAN. The box model is run on the BOXMOX platform using the MOZART4 (Model for Ozone and Related chemical Tracers version 4) chemical mechanism.³⁹ The box model simulates the diurnal variations of chemical species. We ran it for 48 h with the first 24 h as a spin-up. We used the box model to simulate ozone exceedance days in July 2020 by constraining the model with available input data from the ozone exceedance days.

We configured the box model for the Advanced Science Research Center (ASRC) Rooftop Observatory on the City College of New York (CCNY) campus, an intensive urban air-quality monitoring site in Manhattan where difference between NYC-MEGAN and CMAQ-BEIS is the largest (Figure 4c). Modeled isoprene concentrations are most sensitive to isoprene emissions, boundary layer height, and NO (nitric oxide) concentrations in box models.⁴⁰ We constrain our box model with observed boundary layer height and NO_x concentrations to reduce uncertainties and thus to better evaluate NYC-MEGAN isoprene emissions. The boundary layer height was estimated using potential temperature gradients observed by a radiometrics profiling radiometer at CCNY.⁴¹ The summer (June–August) diurnal averages of boundary layer height from 2010 to 2014 were used in the model. The box model was constrained by observed NO_x concentrations for the ozone exceedance days from the CCNY site in the Air Quality System. The CCNY site had concurrent ozone and NO_x measurements and was the closest site to ASRC where isoprene measurements are made (see details below). The observed NO_x concentrations were averaged into hourly data and read into the box model at each model hour. The isoprene emissions were exacted from NYC-MEGAN for the pixel of the measurement site ASRC and averaged into hourly diurnal data for ozone exceedance days.

Other inputs include Ta, PAR, AVOC emissions, and dry deposition velocity. The Ta and PAR were measured by an ATMOS 41 Weather Station at ASRC. We used averaged diurnal Ta and PAR on ozone exceedance days in 2020 to drive the box model. The AVOC emissions were from Knoté et al.³⁹ based on the 2008 National Emission Inventory (NEI). We considered the impact of volatile chemical product (VCP) emissions on ozone production by incorporating emissions/chemistry of methanol, ethanol, acetone, propylene glycol, monoterpenes, and D5-Siloxane.¹⁵ Siloxanes are not included in the current chemical mechanisms MOZART. We mapped siloxane emissions to benzene given their similar reactivity with the hydroxyl radical. The MOZART chemical mechanism in this study lumped the aromatic species benzene, toluene, and xylenes together as the model species TOLUENE. We tuned the emissions of the five VCP species (methanol, ethanol, acetone, monoterpenes, D5-Siloxane) to match the measurements by Cao et al.⁴² with daily mean being 6.6 ppbv, 0.7 ppbv, 1.7 ppbv, 0.6 ppbv, and 1.4 ppbv, respectively. Dry deposition velocities³⁹ were consistent with values used in chemical transport models.⁴³ Note that the box model originally produced higher ozone concentrations than observed for the afternoon (14:00–17:00), despite successfully reproducing the peak ozone concentrations. This discrepancy was mostly likely the result of enhanced mixing due to higher afternoon wind speeds, which box models do not represent. We then tuned the dry deposition velocity of ozone in the early afternoon (from 0.4 cm s⁻¹ to 4.0 cm s⁻¹) to account for this enhanced mixing. This new bulk deposition velocity represents

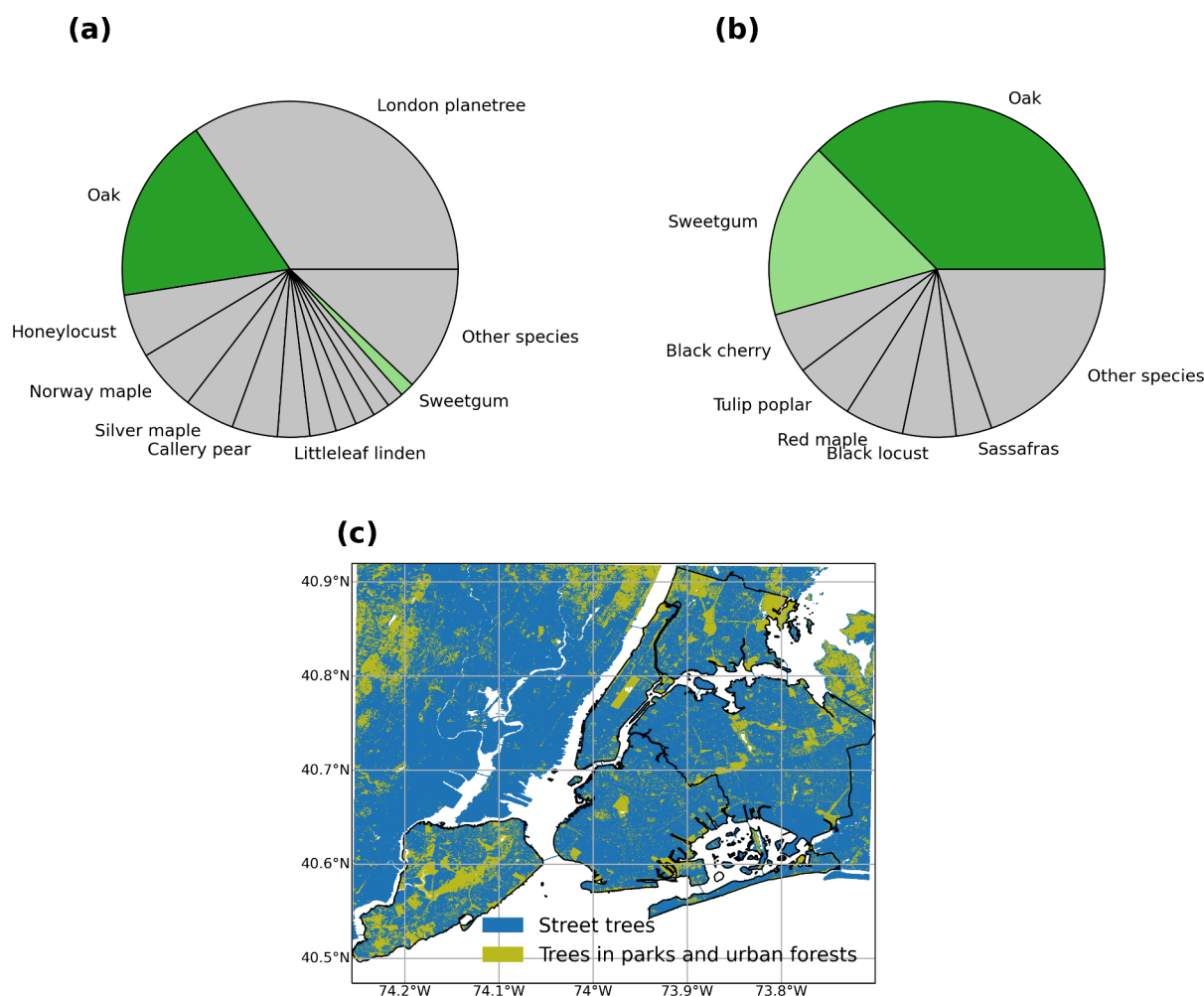


Figure 1. Tree species composition based on basal areas in New York City (NYC) for (a) street trees and (b) trees in parks and urban forests. Two isoprene emitting tree species are highlighted: oak trees (dark green) and sweetgum (light green). (c) Location of street trees and trees in parks and urban forests.

all nonchemical sinks for ozone including enhanced afternoon mixing due to wind speed. The value of 4.0 cm s^{-1} is similar to the upper bound of nonchemical sink strength of ozone derived in forest canopy using one-dimensional mass balance.⁴⁴ The peak ozone concentration was not affected by the tuning of dry deposition. We use peak ozone concentrations in our sensitivity experiments (see details in [Experiments for Future Urban Greening Strategies](#)).

We compared the modeled diurnal variations of isoprene and ozone concentrations for ozone exceedance days with the observations. Isoprene concentrations were measured using on line high-resolution proton-transfer time-of-flight mass spectrometry (HR-PTR-ToF-MS; Ionicon 8000, Analytik GmbH, Austria) at the ASRC in 2020 (see details in Cao et al.⁴²) PTR-ToF-MS is subject to artifacts from ion fragmentation in urban environments, which complicates quantification of key atmospheric VOCs including isoprene.⁴⁵ We corrected the measured isoprene concentrations using the method proposed by Coggon et al.⁴⁵ Measured ozone concentrations were obtained from the CCNY site in the Air Quality System. The observed isoprene and ozone concentrations for the ozone exceedance days in 2020 were averaged into diurnal hourly data and used to evaluate the hourly box model results.

Many different variables, such as boundary layer height, emissions, and chemistry, must be represented correctly for an

observation-based model evaluation to be successful. Because of the lack of concurrent and/or colocated measurements, several limitations are acknowledged with the box model. We used the observation-based diurnal climatology of boundary layer height, which could introduce uncertainties for any given day. The inputs of AVOC emissions are based on the 2008 NEI, which can potentially lead to overestimation AVOC emissions due to strengthened emission controls especially traffic-related VOCs in NYC in recent years. These limitations indicate that the model most likely represents an upper limit of the contribution of AVOCs to ozone production. Sensitivity studies show the uncertainties associated with changes in AVOC emissions are within 5% and do not affect the isoprene emissions and their impacts on ozone (not shown). Two components of oxygenated VCPs, isopropanol and glycerol, are not included in the chemical mechanism. The glycols represent a large fraction of the VCP emissions (>10%) and OH reactivity (>30%),¹⁵ which may lead to underestimation of ozone production from VCPs in the box model. Isopropanol accounts for a small portion of OH reactivity (<5%), and it is unlikely that the uncertainties in missing isopropanol significantly affect our model results on isoprene and ozone concentrations.

Experiments for Future Urban Greening Strategies. NYC has established a citywide goal of equitably reaching at

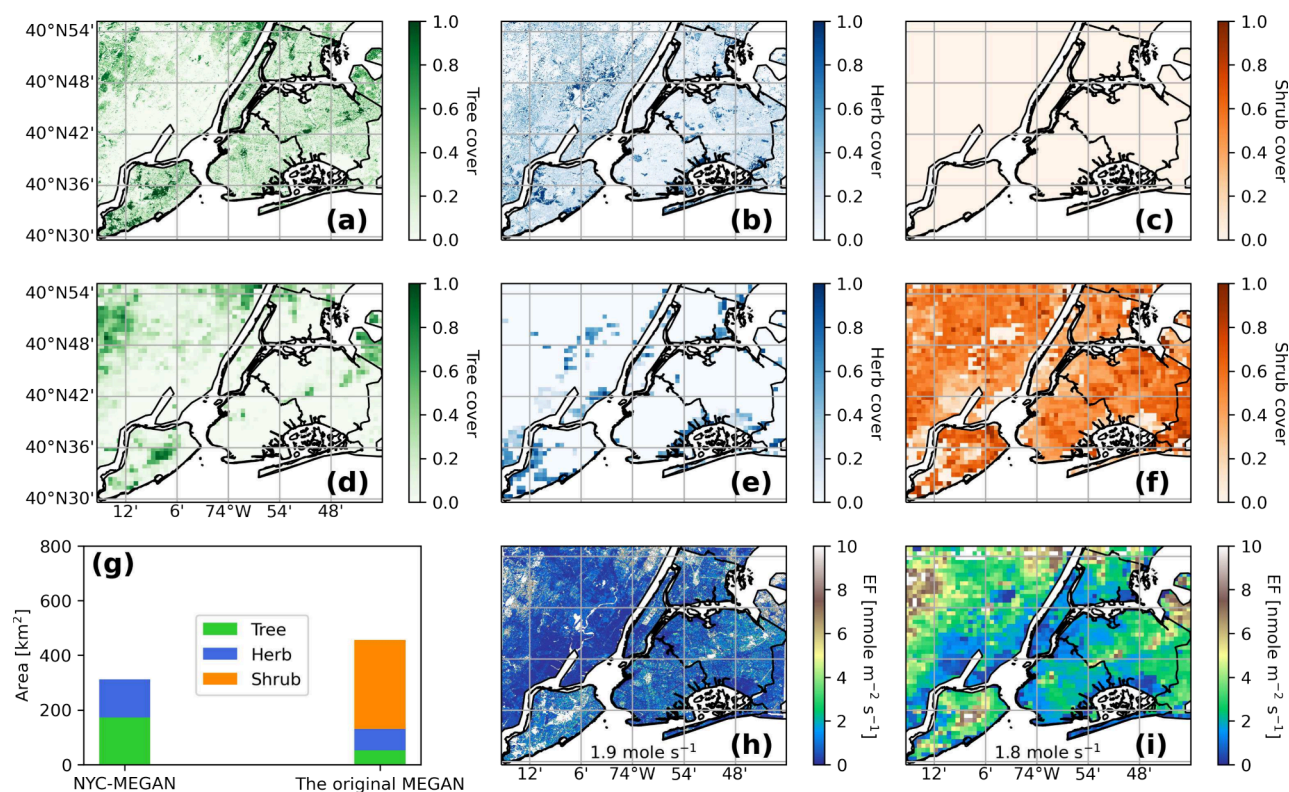


Figure 2. Vegetation cover in NYC. (a–c) Tree, herb, and shrub covers based on the NYC 15 cm land cover map. (d–f) Tree, herb, and shrub covers based on the 1 km land cover map in the original MEGAN. (g) The area (km²) of each vegetation cover in the NYC domain based on the NYC 15 cm land cover map. (h–i) Emission factors (EFs) calculated using the 15 cm land cover map and the 1 km land cover map in the original MEGAN.

least 30% tree cover by 2035. NYC has the potential to increase citywide tree canopy cover from 22% to 42% without changing existing landscape constraints.³⁴ On a borough level, the potential for increasing canopy cover is greatest in Queens (from 19% to 43%) and the smallest is in Manhattan (from 21% to 29%). The Bronx (from 25% to 42%), Brooklyn (from 18% to 32%), and Staten Island (from 31% to 59%) are in between.³⁴

We use NYC-MEGAN and the box model to evaluate the influence of different urban greening scenarios (i.e., variations in species planted) on future isoprene emissions and air quality with a focus on examining peak ozone concentrations. We implemented two different urban greening strategies in NYC-MEGAN to estimate the potential increases in future isoprene emissions: (i) we increased tree canopy cover by expanding tree canopy extent on a borough level while keeping tree species composition unchanged; (ii) we increased tree canopy cover by expanding tree canopy extent on a borough level and assumed the additional canopies are oak.

To evaluate the influence of urban greening on ozone production, we incorporate the potential future isoprene emission changes for the borough of Manhattan (i.e., 1.4–2.2 times more, Figure 5a) in the box model and run it with different NO_x concentrations that represent a range of environments from remote forests to highly polluted cities (i.e., daily average NO_x of 0.1–16 ppbv).

RESULTS AND DISCUSSION

In *Characterization of Land Covers in NYC*, we present the characterization of land covers (i.e., tree species composition, vegetation cover, leaf area index) in NYC. In *High Spatial*

Resolution Isoprene Emissions for NYC, we show the isoprene emissions estimated by NYC-MEGAN that incorporates these land cover data. We compare them with another widely used biogenic emission inventory BEIS. We also evaluate our isoprene emission estimates with rooftop measurements using a box model. In *Influences of Future Urban Greening Strategies on Air Quality*, we estimate future isoprene emissions by implementing plausible greening strategies in NYC-MEGAN. We then show how these future isoprene emission scenarios impact ozone levels using the box model.

Characterization of Land Covers in NYC. Tree Species Composition. Urban ecosystems (e.g., fragmented forests, urban savannas, etc.) are different from natural ecosystems (e.g., intact forests, grasslands, etc.). In urban planning, different trees are planted in different locations for aesthetics and their ecosystem services. Three main locations of urban vegetation can be distinguished: street trees, parks and private garden trees, and urban forest trees.^{46,47} Street trees are exposed to a relatively high stress level (e.g., polluting agents, mechanical damage, shading, local wind gusts, excessive heat, restricted space for crown development, small root volumes, etc.) and typically die much younger than a forest tree.⁴⁸ Park trees and trees in urban forests are exposed to less stressful conditions than street trees and have longer lifespans. Therefore, different tree species composition is expected between street trees and park trees. We consider two ecosystems in NYC-MEGAN: (i) street trees; and (ii) parks/urban forests (referred to as park trees hereafter for simplicity).

Common urban tree genera include cherry (*Prunus*), honey locust (*Gelditsia*), maple (*Acer*), oak (*Quercus*), and sweetgums

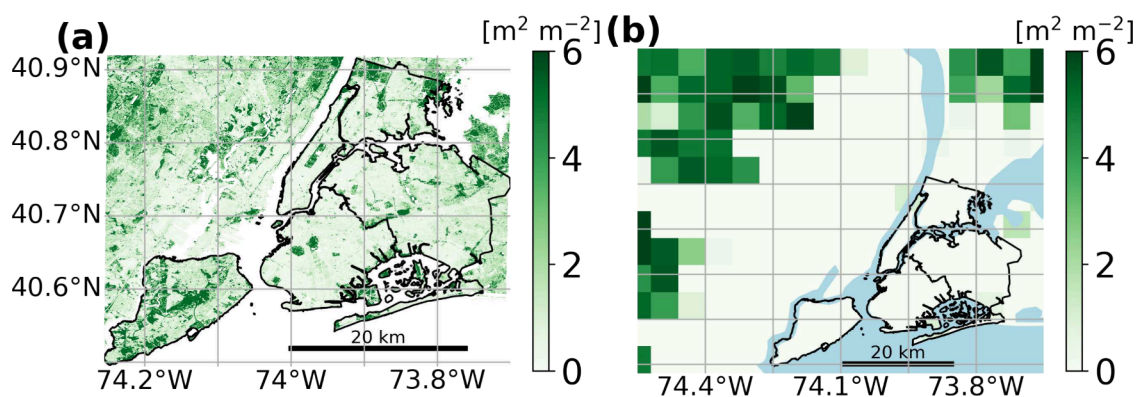


Figure 3. Leaf area index (LAI) in NYC. (a) 30 m spatial resolution Landsat LAI. (b) 1 km spatial resolution LAI compiled for the original MEGAN. Note that panel (b) is a larger area in order to show significant LAI values outside of NYC.

(*Liquidambar*) in the Northeastern US, together accounting for over half of the trees planted.⁴⁹ Among those, oak (*Quercus* spp.) and sweetgum (*Liquidambar styraciflua* L.) are major isoprene emitters.

Street tree species composition is different than the composition of park trees in NYC (Figure 1a,b). In total, 666,134 street trees have been mapped in NYC, covering 132 species. Oak trees account for 18% of all street tree basal areas, with pin oak being the dominant oak species (15%) (Figure 1a). The most abundant street tree is London Planetrees (34% of basal area), a low isoprene-emitter compared to oak genera that emits ~ 800 times more isoprene at standard conditions of temperature and light (i.e., 30 °C; 1000 $\mu\text{mol m}^{-2} \text{s}^{-1}$ of photosynthetically active radiation).⁵⁰ Sweetgum comprises only a small proportion of total street tree basal area. Street trees are widely distributed across the NYC domain, e.g., along streets in the urban core Manhattan, and less dense residential areas of Queens and Brooklyn (Figure 1c). For the park tree ecosystem, over half of the total park tree basal areas are dominated by oaks (37%) and sweetgum (17%) (Figure 1b). Tree species comprising the remaining 46% of basal area are either non- or low-isoprene emitters. Parks and urban forests are found across all NYC boroughs and comprise most of the city's tree canopy cover (Figure 1c), indicating large potential isoprene emissions in parks and urban forests in NYC.

Vegetation Cover. MEGAN considers four vegetation types, trees, herbs, shrubs, and crops. Substantial differences in tree, herb, and shrub covers are found between the 15 cm land cover map in NYC-MEGAN and the 1 km land cover map in original MEGAN (Figure 2). The 15 cm map shows 3.3 times greater tree canopy cover than the 1 km map (i.e., 173 km^2 versus 53 km^2) (Figure 2a,e,i). The 15 cm map represents trees in major parks as well as street trees, while the 1 km map misses most of the street trees and shows smaller tree covers for parks, suggesting that higher spatial resolution land cover is required to adequately simulate urban ecosystem fluxes for street trees and fragmented urban forests. Trees are the largest isoprene contributors to EF in MEGAN, compared to other vegetation types. The higher tree cover suggested by the 15 cm land cover map is one of the main factors driving the differences in EF between the NYC-MEGAN and the original MEGAN. A shrub cover of 42% (326 km^2) is assumed by the 1 km map in original MEGAN. Because shrubs can have a nontrivial emission factor of 4 $\text{nmol m}^{-2} \text{s}^{-1}$ (as a reference point, oak's EF is 33 $\text{nmol m}^{-2} \text{s}^{-1}$), the high shrub cover contributes to 60% of total EF in original MEGAN. The 15 cm

land cover map considers any vegetation less than 2.44 m tall as grass or shrub without differentiating them. However, the tree survey data²⁹ suggests the presence of few shrubs. Therefore, we assume the grass/shrub identified by the 15 cm land cover map are all grass (e.g., zero shrubs). Therefore, the 15 cm land cover map indicates herb cover of 18% (139 km^2) while the 1 km map estimates virtually zero. Because herbaceous plants are assumed to be very low isoprene emitting in MEGAN with an emission factor of 1.0 $\text{nmol m}^{-2} \text{s}^{-1}$, the difference in herb covers between the two maps does not contribute to large differences in EF estimation (Figure 2g,k). Note that *Phragmites* (*Phragmites australis*) has become a ubiquitous part of NYC's landscape and are not included in NYC-MEGAN. It is a non-native perennial grass fringing many freshwater and brackish wetlands across NYC and the study domain. *Phragmites* emits isoprene at a rate of 5–10 $\text{nmol m}^{-2} \text{s}^{-1}$ at 30 °C leaf temperature and can emit up to 25 $\text{nmol m}^{-2} \text{s}^{-1}$ at higher leaf temperatures.⁵¹ Future studies on BVOC emissions in the region should take into account this important invasive grass.

Most BVOC emission models use grid-specific emission factors (EFs) to estimate actual emissions, including MEGAN. Grid-specific EFs are estimated based on the tree species composition and vegetation cover in the model grid. Large uncertainties in EF are associated with the representation of land covers by satellite-based products.²¹ The EF in the original MEGAN is based on the global land cover data with a spatial resolution of 1 km. We use a 15 cm spatial resolution land cover map along with detailed tree surveys described above to calculate the EF in NYC-MEGAN (Figure 2), which allows better representation of highly heterogeneous urban land covers. Surprisingly, the total EF in the NYC domain is comparable. However, the NYC-MEGAN EFs show greater spatial variability across the domain, with park tree ecosystems showing 2–3 times higher EF and the street trees showing lower EF in NYC-MEGAN compared to the original MEGAN. This indicates highly variable BVOC emissions across different urban ecosystems and neighborhoods.

Leaf Area Index. LAI is a critical variable for estimating BVOC emissions in MEGAN. It is used to scale up EF from leaf level to larger spatial areas. It also determines the distribution of in-canopy light and temperature. The values of the 30 m LAI for urban forests and major parks are within the range of ground measurement-based LAI for deciduous forests in the Northeastern US⁵² (3–5 $\text{m}^2 \text{m}^{-2}$; Figure 3a). The 30 m LAI for street trees is small but nonzero. The 1 km

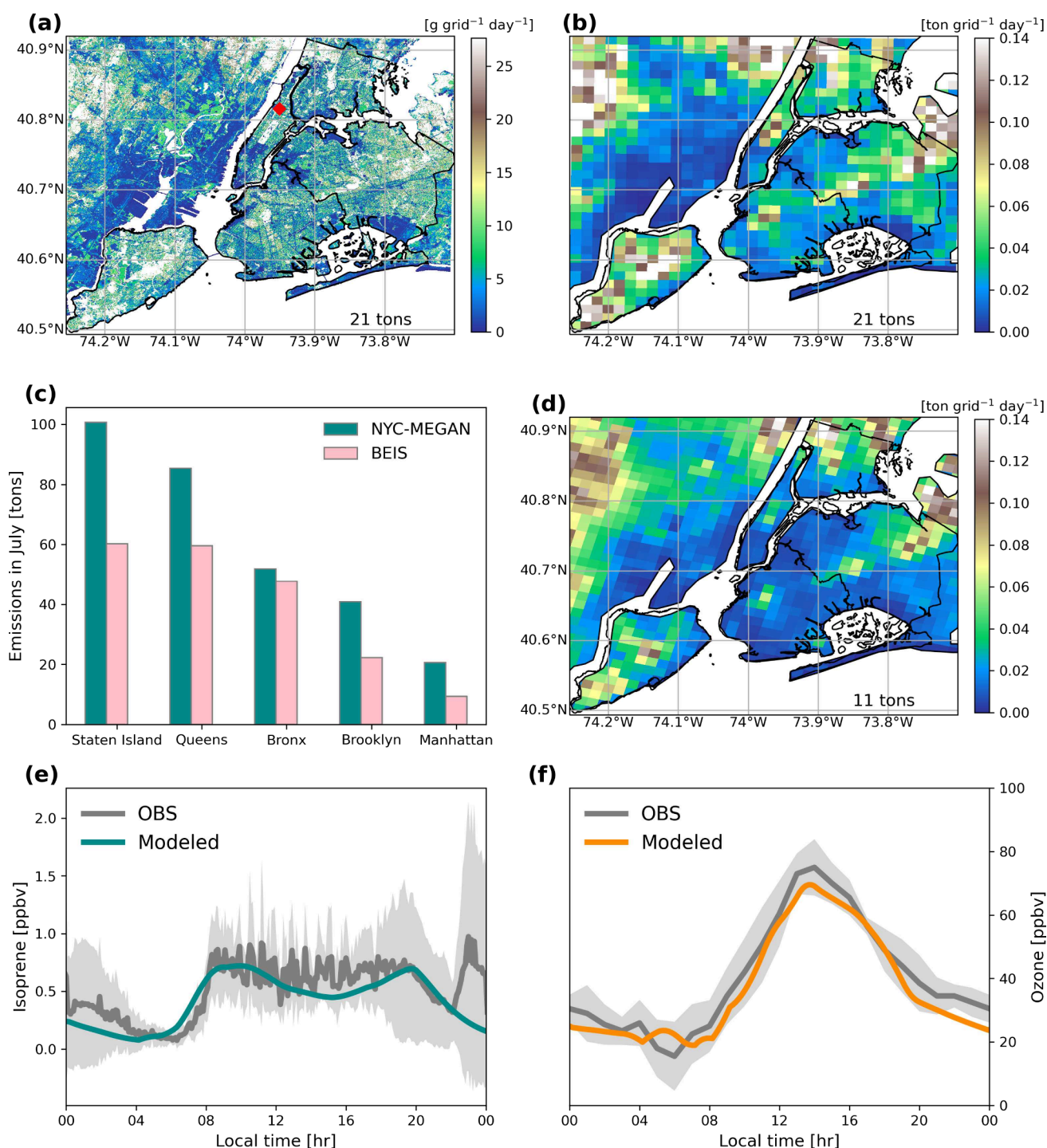


Figure 4. Modeled isoprene emissions in NYC. (a) Modeled daily 30 m isoprene emissions by NYC-MEGAN for July 2, 2018. The 21 tons is the total isoprene emissions in NYC. (b) 30 m NYC-MEGAN daily isoprene emissions resampled to 1.33 km for July 2, 2018. The total mass of isoprene in the domain (21 tons) is the same as panel (a). (c) Modeled monthly total isoprene emissions in July, 2018. (d) Modeled 1.33 km daily isoprene emissions by the Biogenic Emission Inventory System (BEIS) for July 2, 2018. The 11 tons is the total isoprene emissions in NYC. (e, f) Comparison of modeled isoprene and ozone concentrations by the box model with observations for the Advanced Science Research Center (ASRC) Rooftop Observatory in Manhattan on ozone exceedance days. The location of ASRC is noted in panel (a) by the red diamond symbol. Note that the grid area is 30 m \times 30 m in panel (a) and 1.33 km \times 1.33 km in panels (b) and (d).

LAI compiled for the original MEGAN is based on MODIS that has been shown to be inadequate for LAI estimation for urban areas.³⁰ Despite reasonable representation of the more intact natural forests outside NYC, the 1 km LAI map does not meaningfully represent vegetation in NYC (Figure 3b), leading to virtually zero isoprene emissions in NYC in the original

MEGAN. We thus compare our isoprene emissions from NYC-MEGAN with the BEIS in the next section.

High Spatial Resolution Isoprene Emissions for NYC. Comparison of 30 m Isoprene Emissions with the 1.33 km BEIS. There is considerable spatial variability of daily isoprene emissions across the domain, ranging from <5 (e.g., residential

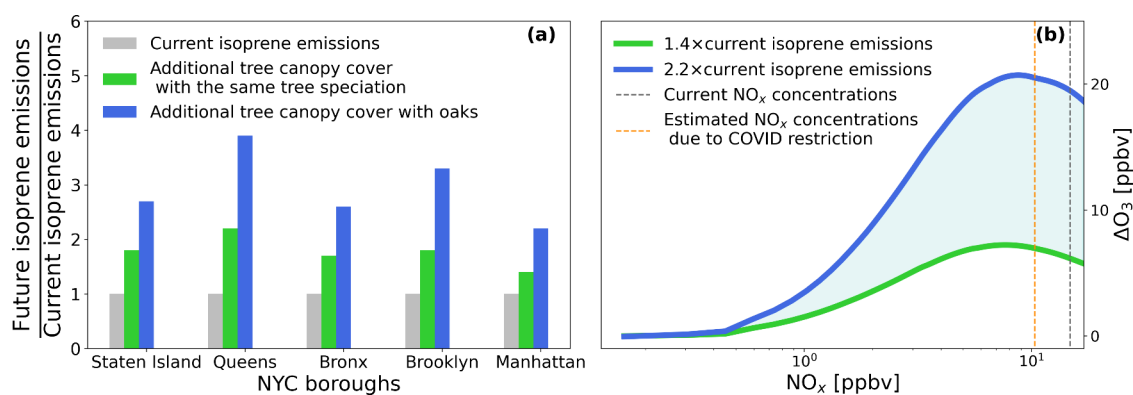


Figure 5. Influence of future urban greening on ozone production. (a) Future isoprene emission estimation for each borough due to likely urban greening scenarios. (b) Changes in peak ozone concentrations due to likely future isoprene emissions for Manhattan in panel (a) under a range of NO_x concentrations. The vertical dashed lines denote current NO_x concentrations in Manhattan (gray) and estimated summer NO_x concentrations due to COVID restriction (orange). The NO_x concentrations are daily averages.

areas in Queens) to $>30 \text{ g grid}^{-1} \text{ day}^{-1}$ (e.g., the urban forests in Staten Island) (Figure 4a). This large spatial heterogeneity is often not captured by large-scale models with coarser spatial resolutions (Figure 4d). The large spatial heterogeneity in isoprene emissions indicates that (i) accurate estimation of BVOC emissions for urban areas requires high spatial resolution data to represent the high heterogeneity in vegetation covers; (ii) measurements of BVOC fluxes from different urban ecosystems (e.g., urban savannas, fragmented forests, etc.) are needed to evaluate model results and improve performance of BVOC emission models in urban landscapes.

BEIS produces less isoprene emissions for major parks and leaves out most of the street trees, resulting in less spatial variability than NYC-MEGAN (Figure 4b). Specifically, parks show higher isoprene emissions in NYC-MEGAN by a factor of 2, due to the large portion of oak and sweetgum in the park trees (Figure 1b) and likely higher LAI (Figure 3a). Street trees also contribute nontrivial amounts of isoprene emissions in NYC-MEGAN. Altogether, the total isoprene emissions in the domain in NYC-MEGAN are almost twice as large as those in BEIS (Figure 4b,d), which appears to follow the tree canopy differences between the 15 cm and the 1 km land cover maps. In summary, the major model differences between the 30 m NYC-MEGAN and the 1.33 km BEIS are most likely due to the inputs including survey-informed tree species composition, vegetation cover based on high-resolution land cover map, and high-resolution LAI, suggesting the need for high-resolution land cover to adequately represent urban ecosystems.

The NYC urban core is still VOC-limited, and understanding the local-scale spatial variability of VOC emissions is crucial for accurate ozone prediction. We compared the total isoprene emissions for July from the two inventories (i.e., NYC-MEGAN and BEIS) for each borough (Figure 4c). Both inventories show that the highest isoprene emissions are from Staten Island and the lowest, from Manhattan. The largest difference between the two inventories occurs in Manhattan with a factor over 2.0, likely due to different emissions from Central Park as well as street trees. Surprisingly, Manhattan has the leafiest streets with an average of 30.9 trees per km of sidewalk, with Queens a close second at 30.7 trees per km, followed by Staten Island (30.4 trees per km), Brooklyn (27.9 trees per km), and the Bronx (23.4 trees per km) (<https://opendata.cityofnewyork.us/data/>). The Bronx has the smallest difference between the two inventories.

MEGAN tends to calculate lower BVOC emissions for urban sites in the eastern US. For example, MEGAN predicts lower daily isoprene average concentrations by a factor of 2–3 than observations at several urban–suburban sites including the New York Botanical Garden Pfizer Plant Research Lab which is located in the Bronx in NYC, likely due to the treatment of vegetation type and/or LAI in the urban/suburban areas.⁵³ Coggon et al.¹⁵ halve isoprene emissions from MEGAN to match the observed isoprene concentrations from the NOAA mobile lab, which produces better model–observation agreement outside NYC but results in an underprediction of isoprene concentrations within the NYC city core. The NYC-MEGAN uses detailed vegetation type and LAI data and produces higher isoprene emissions than BEIS and can potentially reproduce observations of isoprene concentrations in NYC.

Evaluation of 30 m Isoprene Emissions against Measurements. The box model with the NYC-MEGAN isoprene emissions generally captures the temporal evolution and magnitude of isoprene and ozone concentrations (Figure 4e,f). This good agreement highlights that a detailed representation of urban biosphere and knowledge of the spatial and temporal distribution of BVOC emissions are essential to predict variability in ground-level ozone concentrations. The model produces slightly lower isoprene and ozone concentrations in the afternoon than the observed averages. These lower modeled quantities could be due to uncertainties associated with the model's ability to resolve coastal boundary layer dynamics on any given day.

Influences of Future Urban Greening Strategies on Air Quality. Changes in Isoprene Emissions from Urban Greening. Oak trees, major isoprene emitters, are common and recommended in urban tree selection for Northeast US cities due to their tolerance of urban stressors (e.g., heat, drought, ozone pollution, and soil compaction).⁵⁴ Many oak species are also typically included on lists of climate-resilient tree species genera for urban greening in many US cities.^{55,56}

The scenario of planting oaks for additional canopy cover produces the largest increases in isoprene emissions (3–4 times higher in Queens and Brooklyn), whereas increasing tree canopy cover and using the current tree species composition results in the smallest increases in isoprene emissions (i.e., 1.4–2.3 times higher) (Figure 5a). The potential increases in isoprene emissions varies considerably across the five

boroughs, ranging from 1.4 to 4 times, with the largest potential increases in Queens and smallest in Manhattan (Figure 5a).

Changes in Peak Ozone from Increased Isoprene Emissions. Peak ozone from future isoprene emissions is projected to increase by 8–19 ppbv, depending on the urban greening scenarios (Figure 5b). Under the tested scenario of planting oaks for additional canopy cover, NYC would have to dramatically reduce NO_x by a factor of 5 to avoid more severe ozone exceedance events (i.e., <10 ppbv increase in peak ozone). The total reduction in NO_2 concentrations for NYC for the period of 2005–2013 was 40% based on the satellite retrievals.⁵⁷ The large annual reduction rate of $6.7 \pm 1.0\%$ for 2005–2008 has been followed by a much lower rate of $0.8 \pm 1.0\%$ for 2010–2013.⁵⁷ The slowdown in NO_2 reduction is on par with the trends across the Northeastern US for the period of 2011–2015 based on the surface *in situ* NO_2 observations (i.e., $2.6 \pm 2\%$).⁵⁸ If we assume annual reduction rates in NO_2 emissions of 2.0–5.0%, as well as similar emission-concentration patterns for NYC, it would take 30–80 years to reduce NO_2 concentrations enough (i.e., reduced by a factor of 5) to curtail future ozone exceedance events (i.e., peak ozone increases within 10 ppbv) in the context of the urban greening scenario of planting all oaks for the additional canopy cover. Both NYC and New York State have major plans for electrification of buildings and vehicles that are expected to decrease NO_x concentrations within the next 30 years. Stringent lockdown measures following the COVID-19 outbreak resulted in an abrupt decline of 30% in NO_2 emissions from January to May 2020 in NYC.⁵⁹ Assuming similar reduction (i.e., 30%) in NO_x concentrations, the peak ozone increases are similar to those under the current NO_x concentrations. This study provides strong rationale for a comprehensive evaluation of what tree species would be best to target for urban greening plans, balancing the desired ecosystem services with the important role of BVOCs in ozone production.

We run the box model for a site in Manhattan that has similar isoprene increase potential as that in the Bronx or Staten Island (Figure 5a) but greater NO_2 concentrations.⁶⁰ NYC is set to implement congestion pricing in Manhattan south of Central Park in 2024 as a way to reduce travel times on streets and improve public transportation infrastructure. Areas outside the congestion zone may see more traffic congestion and pollution (NO_x) increases—especially in the south Bronx and on the Staten Island Expressway. Similar increases in ozone peaks as Manhattan could be expected for the Bronx or Staten Island in the future. Queens and Brooklyn have lower NO_2 concentrations and higher potentials for urban greening (Figure 5a), so we expect even larger increases in ozone peaks for Queens and Brooklyn than Manhattan on ozone exceedance days in the future as urban greening progresses.

The magnitude of the peak ozone increases (8–19 ppbv) from these future urban greening scenarios is similar to the contribution of total AVOCs to maximum 8 h average ozone in NYC¹⁵ (i.e., up to 20 ppbv). AVOC emissions are expected to continue to decrease with improved vehicle emission controls. The United States Environmental Protection Agency has set strict emissions standards for heavy-duty trucks and buses, taking effect for years 2027 through 2032. The COVID shutdowns in 2020 and 2021 had considerable impacts on ambient VOC concentrations and provided an opportunity to

quantify the reduction in VOCs due to shifts in traffic. The nearly 60% decrease in driving activity was accompanied by 34% reductions in concentrations of benzene (a traffic-related pollutant) concentrations.⁴² Assuming 4 times greater isoprene emissions due to future urban greening and aggressive reductions in AVOCs similar to COVID shutdowns, AVOCs still likely dominate total VOC concentrations in the urban core of NYC. However, due to high reactivity toward ozone, BVOCs would still dominate ozone production and are expected to become increasingly important. While there is some evidence for temperature-dependent AVOC emissions,⁴² BVOC emissions are highly temperature dependent. Increased tree canopy cover is expected to lower the surface temperature, which in turn affects temperature-dependent VOC emissions. Future research of emission inventories is needed to more accurately quantify the relative contribution of BVOCs and AVOCs to ozone production in order to develop effective emission control strategies in polluted urban environments.

CONCLUSIONS AND IMPLICATIONS

This study aims to examine the impact of future urban greening on air quality. We estimated the isoprene emissions in NYC. Accurate estimation of BVOC emissions for urban areas requires high spatial resolution data to represent the heterogeneity in vegetation cover and land cover types. The 30 m NYC-MEGAN driven by high spatial resolution data (i.e., land cover map, tree speciation, and LAI) reveal larger than expected isoprene emissions on hot summer days even in the large, dense NYC that has a relatively low canopy cover of 22%, twice higher than the coarser resolution Biogenic Emission Inventory System (BEIS). The urban tree canopy is highly heterogeneous and includes trees along streets and in parks, yards, and forests. Parks and urban forests show greater isoprene emission strength than street trees because of higher oak/sweetgum composition and tree canopy cover, leading to high spatial variability across NYC. Environmental stresses can vary considerably across an urban landscape. Because environmental conditions (e.g., heat, water stress) can influence BVOC emissions, constraining understanding of the linkages among urban environmental stressors, air pollution and ecological processes that drive BVOC emissions should be a focus of future research.

We evaluated the impact of future urban greening on ozone production. BVOCs drive ozone production on hot summer days, even in mega-cities with large anthropogenic VOC emissions, due to higher reactivity of BVOCs toward ozone formation and high NO_x concentrations in the city. Representing the high spatial heterogeneity in BVOC emissions is crucial for understanding the local-scale spatial and temporal variability of ozone formation on ozone exceedance days, especially if we wish to develop effective mitigation strategies. Our findings suggest that urban greening strategies that favor planting oak trees could increase future isoprene emissions by 1.4–2.2 times in Manhattan, which can result in 8–19 ppbv increases in peak ozone on ozone exceedance days given the current NO_x concentrations. The city would have to dramatically reduce NO_x by a factor of 5 to avoid more severe ozone exceedance events (i.e., <10 ppbv increase in peak ozone) in the context of future urban greening. New York State and NYC are continuing pursuing further NO_x reduction strategies, and these NO_x reductions are already necessary to continue lowering ozone concentrations in NO_x -sensitive regions downwind of NYC. Until we reach the

NO_x reduction goal, BVOCs dominate ozone production on ozone exceedance days.

Increases in urban canopy cover can also lead to other changes regarding air quality. It can increase transpiration and thus lower surface temperature, which in turn affects BVOC emissions as well as mixed layer depth. The additional vegetated surfaces can increase the surface areas available for trace gas and particle deposition, especially ozone dry deposition. Urban greening may impact pollen, depending on the tree species and gender mix. The increased BVOCs can lead to formation of secondary particulate matter. Summertime aerosol composition in NYC is now primarily organic; these oxygenated organic aerosols are formed from an uncertain mix of both biogenic and anthropogenic VOCs, and their emissions show significant temperature dependence.⁶¹ Future increased BVOC and decreased AVOC emissions will likely enhance the biogenic organic aerosol load and its temperature-dependent formation rate. In addition, the coastal areas downwind NYC are exposed to high ozone concentrations due to transport of highly oxidized air from the urban core by sea breezes. Higher ozone concentrations due to future urban greening in the urban core can exacerbate ozone exposure downwind of the city, which could cause slower growth rates of trees⁶² and impact BVOC emissions and thus ozone chemistry where deep NO_x reduction is already taking place. Future studies should target the combined impact of urban greening on air quality using a regional chemical transport model with improved spatial characterization land cover maps and updated anthropogenic emissions based on current policies, as well as surface processes such as vertical mixing and dry deposition. Our findings highlight the complex challenges confronting cities in their efforts to both improve air quality and increase tree canopy cover. We suggest cities develop tree planting palettes that consider the trade-offs between the cooling benefits of trees and their potential influences on air quality in order to optimize the benefits of tree planting efforts on both temperature and air quality.

AUTHOR INFORMATION

Corresponding Author

Dandan Wei – Lamont-Doherty Earth Observatory, Columbia University, Palisades, New York 10027-6902, United States; Environmental Sciences Initiative, City University of New York, Advanced Science Research Center, New York, New York 10031-1246, United States; School of Marine and Atmospheric Science, Stony Brook University, Stony Brook, New York 11794-0701, United States; orcid.org/0000-0002-5597-6233; Email: dandan.wei@stonybrook.edu

Authors

Cong Cao – School of Marine and Atmospheric Science, Stony Brook University, Stony Brook, New York 11794-0701, United States; Present Address: Department of Chemistry, Hong Kong University of Science & Technology, Kowloon, Hong Kong, China; orcid.org/0009-0001-4567-3992

Alexandra Karambelas – Northeast States for Coordinated Air Use Management, Boston, Massachusetts 02114-2014, United States

John Mak – School of Marine and Atmospheric Science, Stony Brook University, Stony Brook, New York 11794-0701, United States; orcid.org/0000-0001-8241-5653

Andrew Reinmann – Environmental Sciences Initiative, City University of New York, Advanced Science Research Center, New York, New York 10031-1246, United States; Graduate Programs in Earth and Environmental Sciences and Biology, City University of New York Graduate Center, New York, New York 10016, United States; Department of Geography and Environmental Science, Hunter College, New York, New York 10065, United States

Róisín Commame – Lamont-Doherty Earth Observatory, Columbia University, Palisades, New York 10027-6902, United States; Department of Earth & Environmental Sciences, Columbia University, New York, New York 10027, United States; orcid.org/0000-0003-1373-1550

Complete contact information is available at:

<https://pubs.acs.org/10.1021/acs.est.4c00495>

Notes

The authors declare no competing financial interest.

ACKNOWLEDGMENTS

We acknowledge support by National Oceanic and Atmospheric Administration under Grant NA20OAR4310306. We thank Arlene Fiore for providing the computing resources. We acknowledge support by the New York State Energy Research and Development Authority (NYSERDA), Agreement No. 101132 (TWO ID No. 161194). NYSERDA has not reviewed the information contained herein, and the opinions expressed in this report do not necessarily reflect those of NYSERDA or the State of New York. We acknowledge Natural Areas Conservancy (NAC) for providing the Upland & Forest Ecological Assessment Data for New York City, 2014 (unpublished raw data).

REFERENCES

- (1) Nuvolone, D.; Petri, D.; Voller, F. The effects of ozone on human health. *Environmental Science and Pollution Research* **2018**, *25*, 8074–8088.
- (2) Lefohn, A. S.; Malley, C. S.; Smith, L.; Wells, B.; Hazucha, M.; Simon, H.; Naik, V.; Mills, G.; Schultz, M. G.; Paoletti, E.; Marco, A. D.; Xu, X.; Zhang, L.; Wang, T.; Neufeld, H. S.; Musselman, R. C.; Tarasick, D.; Brauer, M.; Feng, Z.; Tang, H.; Kobayashi, K.; Sicard, P.; Solberg, S.; Gerosa, G. Tropospheric ozone assessment report: Global ozone metrics for climate change, human health, and crop/ecosystem research. *Elementa: Science of the Anthropocene* **2018**, *6*, 27.
- (3) Jin, X.; Fiore, A.; Boersma, K. F.; Smedt, I. D.; Valin, L. Inferring Changes in Summertime Surface Ozone–NO_x–VOC Chemistry over U.S. Urban Areas from Two Decades of Satellite and Ground-Based Observations. *Environ. Sci. Technol.* **2020**, *54*, 6518–6529.
- (4) Tao, M.; Fiore, A. M.; Jin, X.; Schiferl, L. D.; Commame, R.; Judd, L. M.; Janz, S.; Sullivan, J. T.; Miller, P. J.; Karambelas, A.; Davis, S.; Tzortziou, M.; Valin, L.; Whitehill, A.; Civerolo, K.; Tian, Y. Investigating Changes in Ozone Formation Chemistry during Summertime Pollution Events over the Northeastern United States. *Environ. Sci. Technol.* **2022**, *56*, 15312–15327.
- (5) Wu, S.; Lee, H. J.; Anderson, A.; Liu, S.; Kuwayama, T.; Seinfeld, J. H.; Kleeman, M. J. Direct measurements of ozone response to emissions perturbations in California. *Atmospheric Chemistry and Physics* **2022**, *22*, 4929–4949.
- (6) Tran, T.; Kumar, N.; Knipping, E. Investigating sensitivity of ozone to emission reductions in the New York City (NYC) metropolitan and downwind areas. *Atmos. Environ.* **2023**, *301*, 119675.
- (7) Koplitz, S.; Simon, H.; Henderson, B.; Liljegren, J.; Tonnesen, G.; Whitehill, A.; Wells, B. Changes in Ozone Chemical Sensitivity in

- the United States from 2007 to 2016. *ACS Environ. Au* **2022**, *2*, 206–222.
- (8) Guenther, A.; Karl, T.; Harley, P.; Wiedinmyer, C.; Palmer, P. I.; Geron, C. Estimates of global terrestrial isoprene emissions using MEGAN (Model of Emissions of Gases and Aerosols from Nature). *Atmospheric Chemistry and Physics* **2006**, *6*, 3181–3210.
- (9) Mohamed, M. F.; Kang, D.; Aneja, V. P. Volatile organic compounds in some urban locations in United States. *Chemosphere* **2002**, *47*, 863–882.
- (10) Zhang, Y.; Wang, W.; Wu, S.-Y.; Wang, K.; Minoura, H.; Wang, Z. *Impacts of updated emission inventories on source apportionment of fine particle and ozone over the southeastern U.S.*; Elsevier BV, 2014; Vol. 88; pp 133–154.
- (11) Hou, X.; Strickland, M. J.; Liao, K.-J. Contributions of regional air pollutant emissions to ozone and fine particulate matter-related mortalities in eastern U.S. urban areas. *Environmental Research* **2015**, *137*, 475–484.
- (12) Peng, Y.; Mouat, A. P.; Hu, Y.; Li, M.; McDonald, B. C.; Kaiser, J. Source appointment of volatile organic compounds and evaluation of anthropogenic monoterpene emission estimates in Atlanta, Georgia. *Atmos. Environ.* **2022**, *288*, 119324.
- (13) Duan, C.; Liao, H.; Wang, K.; Ren, Y. The research hotspots and trends of volatile organic compound emissions from anthropogenic and natural sources: A systematic quantitative review. *Environmental Research* **2023**, *216*, 114386.
- (14) Churkina, G.; Kuik, F.; Bonn, B.; Lauer, A.; Grote, R.; Tomiak, K.; Butler, T. M. Effect of VOC Emissions from Vegetation on Air Quality in Berlin during a Heatwave. *Environ. Sci. Technol.* **2017**, *51*, 6120–6130.
- (15) Coggon, M. M.; Gkatzelis, G. I.; McDonald, B. C.; Gilman, J. B.; Schwantes, R. H.; Abuhassan, N.; Aikin, K. C.; Arend, M. F.; Berkoff, T. A.; Brown, S. S.; Campos, T. L.; Dickerson, R. R.; Gronoff, G.; Hurley, J. F.; Isaacman-VanWertz, G.; Koss, A. R.; Li, M.; McKeen, S. A.; Moshary, F.; Peischl, J.; Pospisilova, V.; Ren, X.; Wilson, A.; Wu, Y.; Trainer, M.; Warneke, C. Volatile chemical product emissions enhance ozone and modulate urban chemistry. *Proc. Natl. Acad. Sci. U. S. A.* **2021**, *118* (32), e2026653118.
- (16) Ma, M.; Gao, Y.; Wang, Y.; Zhang, S.; Leung, L. R.; Liu, C.; Wang, S.; Zhao, B.; Chang, X.; Su, H.; Zhang, T.; Sheng, L.; Yao, X.; Gao, H. Substantial ozone enhancement over the North China Plain from increased biogenic emissions due to heat waves and land cover in summer 2017. *Atmospheric Chemistry and Physics* **2019**, *19*, 12195–12207.
- (17) Gu, S.; Guenther, A.; Faiola, C. Effects of Anthropogenic and Biogenic Volatile Organic Compounds on Los Angeles Air Quality. *Environ. Sci. Technol.* **2021**, *55*, 12191–12201.
- (18) Schlaerth, H. L.; Silva, S. J.; Li, Y. Characterizing Ozone Sensitivity to Urban Greening in Los Angeles Under Current Day and Future Anthropogenic Emissions Scenarios. *Journal of Geophysical Research: Atmospheres* **2023**, *128*, e2023JD039199.
- (19) Cai, M.; An, C.; Guy, C. A scientometric analysis and review of biogenic volatile organic compound emissions: Research hotspots, new frontiers, and environmental implications. *Renewable and Sustainable Energy Reviews* **2021**, *149*, 111317.
- (20) Guenther, A. B.; Jiang, X.; Heald, C. L.; Sakulyanontvittaya, T.; Duhl, T.; Emmons, L. K.; Wang, X. The Model of Emissions of Gases and Aerosols from Nature version 2.1 (MEGAN2.1): an extended and updated framework for modeling biogenic emissions. *Geoscientific Model Development* **2012**, *5*, 1471–1492.
- (21) Opacka, B.; Müller, J.-F.; Stavrakou, T.; Bauwens, M.; Sindelarova, K.; Markova, J.; Guenther, A. B. Global and regional impacts of land cover changes on isoprene emissions derived from spaceborne data and the MEGAN model. *Atmospheric Chemistry and Physics* **2021**, *21*, 8413–8436.
- (22) Hardiman, B. S.; Wang, J. A.; Hutyra, L. R.; Gately, C. K.; Getson, J. M.; Friedl, M. A. Accounting for urban biogenic fluxes in regional carbon budgets. *Science of The Total Environment* **2017**, *592*, 366–372.
- (23) Miller, D. L.; Roberts, D. A.; Clarke, K. C.; Lin, Y.; Menzer, O.; Peters, E. B.; McFadden, J. P. Gross primary productivity of a large metropolitan region in midsummer using high spatial resolution satellite imagery. *Urban Ecosystems* **2018**, *21*, 831–850.
- (24) Wei, D.; Reinmann, A.; Schiferl, L. D.; Commane, R. High resolution modeling of vegetation reveals large summertime biogenic CO₂ fluxes in New York City. *Environmental Research Letters* **2022**, *17*, 124031.
- (25) Zhao, K.; Bao, Y.; Huang, J.; Wu, Y.; Moshary, F.; Arend, M.; Wang, Y.; Lee, X. A high-resolution modeling study of a heat wave-driven ozone exceedance event in New York City and surrounding regions. *Atmos. Environ.* **2019**, *199*, 368–379.
- (26) Zhang, J.; Ninneman, M.; Joseph, E.; Schwab, M. J.; Shrestha, B.; Schwab, J. J. Mobile Laboratory Measurements of High Surface Ozone Levels and Spatial Heterogeneity During LISTOS 2018: Evidence for Sea Breeze Influence. *Journal of Geophysical Research: Atmospheres* **2020**, *125* (11), e2019JD031961.
- (27) Couillard, M. H.; Schwab, M. J.; Schwab, J. J.; Lu, C.-H. S.; Joseph, E.; Stutsrim, B.; Shrestha, B.; Zhang, J.; Knepp, T. N.; Gronoff, G. P. Vertical Profiles of Ozone Concentrations in the Lower Troposphere Downwind of New York City During LISTOS 2018–2019. *Journal of Geophysical Research: Atmospheres* **2021**, *126* (23), e2021JD035108.
- (28) University of Vermont Spatial Analysis Laboratory, in collaboration with New York City Department of Information Technology and Telecommunications (NYC DoITT), Applied Geographics (AppGeo), and Quantum Spatial. *High resolution land cover data set for New York City*; 2017.
- (29) Nowak, D. J.; Bodine, A. R.; Hoehn, R. E.; Ellis, A.; Hirabayashi, S.; Coville, R.; Auyeung, D. N.; Sonti, N. F.; Hallett, R. A.; Johnson, M. L.; Stephan, E.; Taggart, T.; Endreny, T. *Urban Forest of New York City*; 2018.
- (30) Kang, Y.; Ozdogan, M.; Gao, F.; Anderson, M. C.; White, W. A.; Yang, Y.; Yang, Y.; Erickson, T. A. A data-driven approach to estimate leaf area index for Landsat images over the contiguous US. *Remote Sensing of Environment* **2021**, *258*, 112383.
- (31) Bezyk, Y.; Sówka, I.; Górka, M. Assessment of urban CO₂ budget: Anthropogenic and biogenic inputs. *Urban Climate* **2021**, *39*, 100949.
- (32) Berland, A.; Shiflett, S. A.; Shuster, W. D.; Garmestani, A. S.; Goddard, H. C.; Herrmann, D. L.; Hopton, M. E. The role of trees in urban stormwater management. *Landscape and Urban Planning* **2017**, *162*, 167–177.
- (33) Rosenzweig, C.; Solecki, W. D.; Parshall, L.; Lynn, B.; Cox, J.; Goldberg, R.; Hodges, S.; Gaffin, S.; Slosberg, R. B.; Savio, P.; Dunstan, F.; Watson, M. Mitigating New York City's Heat Island: Integrating Stakeholder Perspectives and Scientific Evaluation. *Bulletin of the American Meteorological Society* **2009**, *90*, 1297–1312.
- (34) Treglia, M. L.; Piland, N. C.; Leu, K.; Slooten, A. V.; Maxwell, E. N. Understanding opportunities for urban forest expansion to inform goals: Working toward a virtuous cycle in New York City. *Frontiers in Sustainable Cities* **2022**, *4*, 1.
- (35) Wickham, J.; Stehman, S. V.; Sorenson, D. G.; Gass, L.; Dewitz, J. A. Thematic accuracy assessment of the NLCD 2016 land cover for the conterminous United States. *Remote Sensing of Environment* **2021**, *257*, 112357.
- (36) Benjamin, S. G.; Weygandt, S. S.; Brown, J. M.; Hu, M.; Alexander, C. R.; Smirnova, T. G.; Olson, J. B.; James, E. P.; Dowell, D. C.; Grell, G. A.; Lin, H.; Peckham, S. E.; Smith, T. L.; Moninger, W. R.; Kenyon, J. S.; Manikin, G. S. A North American Hourly Assimilation and Model Forecast Cycle: The Rapid Refresh. *Monthly Weather Review* **2016**, *144*, 1669–1694.
- (37) Bash, J. O.; Baker, K. R.; Beaver, M. R. Evaluation of improved land use and canopy representation in BEIS v3.61 with biogenic VOC measurements in California. *Geoscientific Model Development* **2016**, *9*, 2191–2207.
- (38) Torres-Vazquez, A.; Pleim, J.; Gilliam, R.; Pouliot, G. Performance Evaluation of the Meteorology and Air Quality Conditions From Multiscale WRF-CMAQ Simulations for the Long

- Island Sound Tropospheric Ozone Study (LISTOS). *Journal of Geophysical Research: Atmospheres* **2022**, *127* (5), e2021JD035890.
- (39) Knote, C.; Tuccella, P.; Curci, G.; Emmons, L.; Orlando, J. J.; Madronich, S.; Baró, R.; Jiménez-Guerrero, P.; Luecken, D.; Hogrefe, C.; Forkel, R.; Werhahn, J.; Hirtl, M.; Pérez, J. L.; José, R. S.; Giordano, L.; Brunner, D.; Yahya, K.; Zhang, Y. Influence of the choice of gas-phase mechanism on predictions of key gaseous pollutants during the AQMEII phase-2 intercomparison. *Atmos. Environ.* **2015**, *115*, 553–568.
- (40) Wei, D.; Fuentes, J. D.; Gerken, T.; Chamecki, M.; Trowbridge, A. M.; Stoy, P. C.; Katul, G. G.; Fisch, G.; Acevedo, O.; Manzi, A.; von Randow, C.; dos Santos, R. M. N. Environmental and biological controls on seasonal patterns of isoprene above a rain forest in central Amazonia. *Agricultural and Forest Meteorology* **2018**, *256–257*, 391–406.
- (41) Melecio-Vázquez, D.; González-Cruz, J.; Arend, M.; Han, Z.; Gutierrez, E.; Dempsey, M.; Booth, J. New York Metro-Area Boundary Layer Catalogue: Boundary Layer Height and Stability Conditions from Long-Term Observations. *Ninth International Conference on Urban Climate jointly with 12th Symposium on the Urban Environment*; Centre de Congres Pierre Baudis, Toulouse, France, 2015.
- (42) Cao, C.; Gentner, D. R.; Commane, R.; Toledo-Crow, R.; Schiferl, L. D.; Mak, J. E. Policy-Related Gains in Urban Air Quality May Be Offset by Increased Emissions in a Warming Climate. *Environ. Sci. Technol.* **2023**, *57*, 9683–9692.
- (43) Zhang, L.; Brook, J. R.; Vet, R. A revised parameterization for gaseous dry deposition in air-quality models. *Atmospheric Chemistry and Physics* **2003**, *3*, 2067–2082.
- (44) Freire, L. S.; Gerken, T.; Ruiz-Plancarte, J.; Wei, D.; Fuentes, J. D.; Katul, G. G.; Dias, N. L.; Acevedo, O. C.; Chamecki, M. Turbulent mixing and removal of ozone within an Amazon rainforest canopy. *Journal of Geophysical Research: Atmospheres* **2017**, *122*, 2791–2811.
- (45) Coggon, M. M.; Stockwell, C. E.; Clafin, M. S.; Pfannerstill, E. Y.; Lu, X.; Gilman, J. B.; Marcantonio, J.; Cao, C.; Bates, K.; Gkatzelis, G. I.; Lamplugh, A.; Katz, E. F.; Arata, C.; Apel, E. C.; Hornbrook, R. S.; Piel, F.; Majluf, F.; Blake, D. R.; Wisthaler, A.; Canagaratna, M.; Lerner, B. M.; Goldstein, A. H.; Mak, J. E.; Warneke, C. Identifying and correcting interferences to PTR-ToF-MS measurements of isoprene and other urban volatile organic compounds. *Atmos. Meas. Tech.* **2024**, *17*, 801.
- (46) Sæbø, A.; Benedikz, T.; Randrup, T. B. Selection of trees for urban forestry in the Nordic countries. *Urban Forestry & Urban Greening* **2003**, *2*, 101–114.
- (47) Sæbø, A.; Borzan, Ž.; Ducatillon, C.; Hatzistathis, A.; Lagerström, T.; Supuka, J.; García-Valdecantos, J. L.; Rego, F.; Slycken, J. V. *Urban Forests and Trees*; Springer: Berlin Heidelberg, 2005; pp 257–280.
- (48) Smith, I. A.; Dearborn, V. K.; Hutyrá, L. R. Live fast, die young: Accelerated growth, mortality, and turnover in street trees. *PLoS One* **2019**, *14*, e0215846.
- (49) Doroski, D. A.; Ashton, M. S.; Duguid, M. C. The future urban forest – A survey of tree planting programs in the Northeastern United States. *Urban Forestry & Urban Greening* **2020**, *55*, 126816.
- (50) Curtis, A.; Helmig, D.; Baroch, C.; Daly, R.; Davis, S. Biogenic volatile organic compound emissions from nine tree species used in an urban tree-planting program. *Atmos. Environ.* **2014**, *95*, 634–643.
- (51) Velikova, V.; Pinelli, P.; Loreto, F. Consequences of inhibition of isoprene synthesis in *Phragmites australis* leaves exposed to elevated temperatures. *Agriculture, Ecosystems & Environment* **2005**, *106*, 209–217.
- (52) Zhao, F.; Yang, X.; Schull, M. A.; Román-Colón, M. O.; Yao, T.; Wang, Z.; Zhang, Q.; Jupp, D. L.; Lovell, J. L.; Culvenor, D. S.; Newnham, G. J.; Richardson, A. D.; Ni-Meister, W.; Schaaf, C. L.; Woodcock, C. E.; Strahler, A. H. Measuring effective leaf area index, foliage profile, and stand height in New England forest stands using a full-waveform ground-based lidar. *Remote Sensing of Environment* **2011**, *115*, 2954–2964.
- (53) Wang, P.; Schade, G.; Estes, M.; Ying, Q. Improved MEGAN predictions of biogenic isoprene in the contiguous United States. *Atmos. Environ.* **2017**, *148*, 337–351.
- (54) Sjomán, H.; Busse Nielsen, A. Selecting trees for urban paved sites in Scandinavia – A review of information on stress tolerance and its relation to the requirements of tree planners. *Urban Forestry & Urban Greening* **2010**, *9*, 281–293.
- (55) Roloff, A.; Korn, S.; Gillner, S. The Climate-Species-Matrix to select tree species for urban habitats considering climate change. *Urban Forestry & Urban Greening* **2009**, *8*, 295–308.
- (56) Cannon, C. H.; Petit, R. J. The oak syngameon: more than the sum of its parts. *New Phytologist* **2020**, *226*, 978–983.
- (57) Lamsal, L. N.; Duncan, B. N.; Yoshida, Y.; Krotkov, N. A.; Pickering, K. E.; Streets, D. G.; Lu, Z. U.S. NO₂ trends (2005–2013): EPA Air Quality System (AQS) data versus improved observations from the Ozone Monitoring Instrument (OMI). *Atmos. Environ.* **2015**, *110*, 130–143.
- (58) Jiang, Z.; McDonald, B. C.; Worden, H.; Worden, J. R.; Miyazaki, K.; Qu, Z.; Henze, D. K.; Jones, D. B. A.; Arellano, A. F.; Fischer, E. V.; Zhu, L.; Boersma, K. F. Unexpected slowdown of US pollutant emission reduction in the past decade. *Proc. Natl. Acad. Sci. U. S. A.* **2018**, *115*, 5099–5104.
- (59) Tzortziou, M.; Kwong, C. F.; Goldberg, D.; Schiferl, L.; Commane, R.; Abuhassan, N.; Szykman, J. J.; Valin, L. C. Declines and peaks in NO₂ pollution during the multiple waves of the COVID-19 pandemic in the New York metropolitan area. *Atmospheric Chemistry and Physics* **2022**, *22*, 2399–2417.
- (60) Kheirbek, I.; Johnson, S.; Ito, K.; Anan, K.; Huskey, C.; Matte, T.; Kass, D.; Eisl, H.; Gorczynski, J.; Markowitz, S. *The New York City Community Air Survey: Neighborhood Air Quality 2008–2014*; 2016.
- (61) Hass-Mitchell, T.; Joo, T.; Rogers, M.; Nault, B. A.; Soong, C.; Tran, M.; Seo, M.; Machesky, J. E.; Canagaratna, M.; Roscioli, J.; Clafin, M. S.; Lerner, B. M.; Blomdahl, D. C.; Misztal, P. K.; Ng, N. L.; Dillner, A. M.; Bahreini, R.; Russell, A.; Krechmer, J. E.; Lambe, A.; Gentner, D. R. Increasing Contributions of Temperature-Dependent Oxygenated Organic Aerosol to Summertime Particulate Matter in New York City. *ACS ES&T Air* **2024**, *1*, 113–128.
- (62) Gregg, J. W.; Jones, C. G.; Dawson, T. E. Urbanization effects on tree growth in the vicinity of New York City. *Nature* **2003**, *424*, 183–187.